

Radiation shielding materials and radiation scatter effects for interventional radiology (IR) physicians

J. P. McCaffrey,^{a)} F. Tessier, and H. Shen

Institute for National Measurement Standards, National Research Council of Canada, Building M-35, 1200 Montreal Road, Ottawa K1A 0R6, Canada

(Received 8 March 2012; revised 6 June 2012; accepted for publication 7 June 2012; published 3 July 2012)

Purpose: To measure the attenuation effectiveness and minimize the weight of new non-Pb radiation shielding materials used for radiation protection by interventional radiology (IR) physicians, to compare the accuracy of the different standard measurement geometries of these materials, and to determine x-ray qualities that correspond to the scattered radiation that IR physicians typically encounter.

Methods: Radiation attenuation capabilities of non-Pb materials were investigated. Typically, most studies of non-Pb materials have focused on the attenuating properties of metal powders. In this study, layers of materials incorporating non-Pb powdered compounds such as Bi_2O_3 , Gd_2O_3 , and BaSO_4 were measured individually, as bilayers, and as a Bi_2O_3 -loaded hand cream. Attenuation measurements were performed in narrow-beam (fluorescence excluded) and broad beam (fluorescence included) geometries, demonstrating that these different geometries provided significantly different results. The Monte Carlo (MC) program EGSnrc was used to calculate the resulting spectra after attenuation by radiation shielding materials, and scattered x-ray spectra after 90° scattering of eight ASTM Standard primary x-ray beams. Surrogate x-ray qualities that corresponded to these scattered spectra were tabulated.

Results: Radiation shielding materials incorporating Bi_2O_3 were found to provide equivalent or superior attenuation compared with commercial Pb-based and non-Pb materials across the 60–130 kVp energy range. Measurements were made for single layers of the Bi_2O_3 compound and for bilayers where the ordering was low atomic number (Z) layer closest to x-ray source/high Z (Bi_2O_3) layer farthest from the x-ray source. Narrow-beam Standard test methods which do not include the contribution from fluorescence overestimated the attenuating capabilities of Pb and non-Pb materials. Measurements of a newly developed, quick-drying, and easily removable Bi_2O_3 -loaded hand cream demonstrated better attenuation capabilities than commercial Bi_2O_3 -loaded gloves. Scattered radiation measurements and MC simulations illustrated that the spectra resulting from 90° scattering of primary x-ray beam qualities can be approximated by surrogate x-ray qualities which are more representative of the radiation actually encountered by IR physicians. A table of surrogate qualities of the eight ASTM F2547-06 Standard qualities was compiled.

Conclusions: New non-Pb compound materials, particularly single layers or bilayers incorporating Bi_2O_3 , can reduce the weight of radiation protection materials while providing equivalent or better protection compared to Pb-based materials. Attenuation measurements in geometries that exclude the contribution from fluorescence substantially underestimate the quantity of transmitted radiation. A new Bi_2O_3 -loaded hand cream demonstrated a novel and effective approach for hand protection. Standard testing protocols for radiation protection materials used by IR physicians specify a wider kVp range than is necessary. A more realistic range would acknowledge the lower kVp resulting from scatter and allow IR physicians to confidently utilize lighter-weight materials while still receiving adequate protection. Standards protocols incorporating the adjustments described in this work would maintain the safety of IR personnel and lessen the physical repercussions of long hours wearing unnecessarily heavy radiation protection garments. © 2012 American Association of Physicists in Medicine. [<http://dx.doi.org/10.1118/1.4730504>]

Key words: ionizing radiation, radiation shielding, radiation scatter, broad beam

I. INTRODUCTION

Interventional radiology (IR) procedures include an inherent risk of radiation exposure to both physicians and patients.^{1–11} For longer procedures such as coronary interventions, peripheral vascular interventions, heart catheter, angiography, etc.,

the dose received by physicians and attendant staff is almost entirely attributable to radiation scattered from the patient.^{7,9} Not surprisingly, an industry has arisen to supply radiation protection garments to these physicians. Traditionally, these garments have been made by incorporating powdered lead (Pb) in a flexible polymer matrix. The more recent demand

for non-Pb radiation protection garments to avoid hazardous material disposal issues has resulted in the production of materials that incorporate one or more less toxic metal powders into polymer layers.^{12–18}

Many radiation protection garments tend to be uncomfortably heavy if worn for long periods. A moderate reduction in weight can result from using appropriate non-Pb materials, providing a second major motivation for investigating non-Pb materials for radiation protection. Measurements and calculations show that, depending on the photon energy, some non-Pb materials can provide more effective radiation attenuation than Pb-based materials per unit weight, particularly in the keV region above the non-Pb metal's K-absorption edge.¹⁹ At mean x-ray photon energies below approximately 45 keV, these materials can provide slightly more effective attenuation per unit mass than even pure Pb.¹⁹ Bilayers (two different layers of radiation attenuating material stacked together, with the material containing the lower-Z metal positioned closest to the radiation source) can significantly improve the attenuation per unit weight of a radiation protection garment. Through judicious application of the characteristics of the photoelectric effect, bilayers have been shown to provide significantly better attenuation per unit mass than Pb-based materials, and substantially more effective attenuation per unit mass than even pure Pb over a broad energy range up to mean photon energies of at least 66 keV.²⁰

A significant challenge in determining the characteristics of Pb-based and non-Pb-based radiation shielding materials is that different manufacturers using the same non-Pb material (Sb, for example) will produce radiation protection materials that vary significantly in their attenuation capabilities. General principles can be gleaned from theory and calculations, but the performance of a particular material from a particular manufacturer must be verified by measurements. The measurements given in this paper, while they apply only to the specific materials provided for these studies, are meant to provide suggestions and insights for obtaining reliable attenuation measurements of radiation shielding materials from any source.

This paper is the third in a series investigating non-Pb radiation protection materials. The first paper¹⁹ investigated the possibilities and problems inherent in the use of non-Pb metals embedded in polymer sheets for radiation shielding garments. The second paper²⁰ addressed improvements in radiation attenuation provided by application of the photoelectric effect through the use of bilayers, which can maintain a more consistent improvement in attenuation across the full spectrum. For completeness, this third paper continues the investigation of new radiation protection materials introduced on the market since the publication of the earlier papers. These new materials are based on powdered metallic compounds (as opposed to metal powders) incorporated into polymer sheets. However, the bulk of this paper is concerned with other related issues that arose as a result of the measurements and calculations described in the first two papers. These new investigations include:

- (a) a comparison of narrow beam versus broad beam measurement geometries for radiation shielding materials and the effect of fluorescence on these measurements,
- (b) the effectiveness of a novel Bi₂O₃-loaded hand cream in comparison with Bi₂O₃-loaded gloves, and
- (c) a discussion of the actual x-ray spectra IR physicians typically encounter due to x-ray scatter in contrast to contact with direct x-ray beams. Monte Carlo (MC) calculations were employed to determine surrogate beams—substitute x-ray qualities that provide a reasonable approximation of the actual scattered x-ray spectra encountered at the front of a water phantom after incident spectra (in this case the eight ASTM F2547-06 Standard qualities) were scattered at 90° from a second water phantom positioned at a 45° angle to the direct beam.

Pure metal layers are more effective attenuators than materials incorporating powdered metals imbedded in a polymer matrix because the polymer adds weight but little attenuation, so heavier layers of these metal-imbedded polymer materials are needed to provide the same attenuation as the pure metal. The most successful manufacturers have developed processes which provide the highest loading of metal powder while maintaining the required flexibility of the material. Recently, several companies have developed (or are in the process of developing) polymers loaded with powdered metallic compounds such as Bi₂O₃, Gd₂O₃, and BaSO₄ to take advantage of their potentially useful attenuating capabilities. One manufacturer²¹ has been particularly successful in developing their process for Bi₂O₃-loaded polymers, including a novel Bi₂O₃-loaded hand cream.

With new products being generated by many different manufacturers, radiation attenuation Standards are becoming increasingly important for evaluating attenuation capabilities. There are currently several Standards for measuring the attenuation capabilities of these products. For example,

- ASTM F 2547-06 Standard test method for determining the attenuation properties in a primary x-ray beam of materials used to protect against radiation generated during the use of x-ray equipment,²²
- DIN 6857 radiation protection accessories for medical use of x-rays—Part 1: Determination of shielding properties of unleaded or lead reduced protective clothing,²³
- IEC 61331-1 protective devices against diagnostic medical x-radiation—Part 1: Determination of attenuation properties of materials.²⁴

Unfortunately, these Standards do not recommend common, consistent procedures for measuring the attenuation of x-rays by protective materials over a variety of accelerating potential ranges and for different measurement geometries. One of the more important differences, measurement geometry, is discussed in Secs. II and III below. For all measurements described in this paper, we utilize an inverse broad beam geometry similar to that described in DIN 6857. All incident x-ray beam qualities utilized in this study were

primary standard medium energy x-ray beams provided by the Ionizing Radiation Standards laboratories at the National Research Council of Canada in Ottawa, Canada.

The Standards refer to the concept of “lead (Pb) equivalency,” which is the thickness in millimeters of high-purity (>99.9%) Pb for which the radiation protection material must provide the same attenuation; i.e., the transmitted air kerma must be equal. For example, “0.25 mm Pb equivalent material” must provide the same attenuation (same quantity of transmitted air kerma) as 0.25 mm of pure Pb at a specified x-ray quality. However, the effectiveness of all metals as attenuators vary with photon energy, and a non-Pb element or combination of elements can exceed the attenuation capabilities of Pb at some energies but be less effective at others, due to the photoelectric effect.

The ASTM Standard F2547-06 recommends eight x-ray qualities from 60 to 130 kVp for radiation attenuation measurements. These eight qualities are used as reference qualities throughout the current study since they span in small steps the energy range used for the bulk of medical x-ray imaging, excluding mammography. In this energy range, the photoelectric effect is dominant for the metals used in radiation protection garment materials. Figure 1(a) displays the transmitted spectra of four of the eight ASTM International Standard F2547-06 radiation qualities (varied in amplitude for clarity) after attenuation by 0.25 mm Pb, as calculated by the EGSnrc user codes *BEAMnrc* and *cavity*.^{25,26} The narrow peaks at approximately 59 and 67 keV are tungsten (W) $K\alpha$ and $K\beta$ emission peaks appearing as a result of fluorescence from the W anode in the x-ray tube, and the narrow peaks at approximately 74 and 85 keV are Pb $K\alpha$ and $K\beta$ emission peaks appearing as a result of fluorescence from the 0.25 mm thick Pb sheet. These spectra were calculated with the detector mounted against the Pb sheet to include fluorescence (discussed in detail in Sec. II.A.)

For the ASPM 60 (and 70) kVp spectra, the shape of the spectrum consists of a simple continuous curve. Beginning at the 80 kVp quality, tungsten $K\alpha$ and $K\beta$ emission peaks appear. For the qualities from 100 to 130 kVp, the effects of the K-absorption edge for Pb become apparent with the sharp drop in intensity at 88 keV, and the Pb $K\alpha$ and $K\beta$ emission peaks becoming increasingly stronger.²⁷

Measurements of the eight ASTM qualities through 0.25 mm Pb varies from about 0.3% total air kerma transmittance for the 60 kVp quality to approximately 8% transmittance for the 130 kVp quality [Fig. 1(b)]. The 60 and 70 kVp data points in this figure reflect the simple spectral shape of the 60 kVp spectrum as shown in Fig. 1(a), while the data points for the higher kVps reflect the additional fluence contributed by the W and Pb $K\alpha$ and $K\beta$ emission peaks and the effects of the Pb K-absorption edge. A line has been drawn through the data points representing the simple spectral shapes for 60 and 70 kVp in Fig. 1(b) to emphasize the additional fluence resulting from the more complex spectral shapes at the higher kVps. In general, the higher the kVp, the more attenuating material and weight are required to provide the desired percentage of attenuation. With all Pb or non-Pb

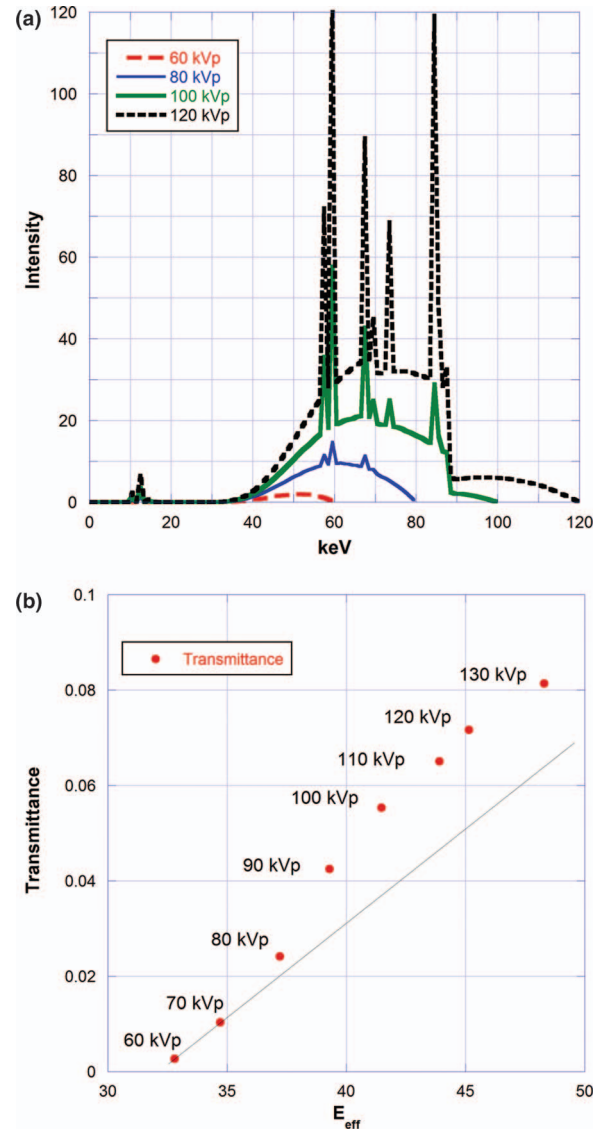


FIG. 1. (a) Transmitted spectra of four of the eight ASTM International Standard F2547-06 x-ray qualities, to demonstrate variation in spectral shape. (b) Relative transmittance of the eight ASTM qualities with 0.5 mm Pb attenuation.

metals, there are anomalies introduced in the x-ray fluence near the K-absorption edge energies and emission peaks for those specific metals.

As an example, in a facility employing a 130 kVp x-ray tube where an acceptable minimum level of radiation protection was deemed to be 8% total air kerma transmittance [92% attenuation, as taken from Fig. 1(b)], 0.5 mm of Pb equivalent radiation attenuation material would be appropriate. Pure Pb shielding would weigh 0.568 g/cm², so an apron that required an area of 1.0 m² of 0.5 mm Pb equivalent material would weigh at least 5.7 kg. For a facility with an 80 kVp x-ray tube, limiting the transmission to the same 8% would require only 0.25 mm Pb equivalent material, so a similar 1.0 m² apron would weigh only half as much as the 0.5 mm Pb equivalent apron. The average weight of a typical commercial one-piece 0.5 mm Pb equivalent radiation shielding apron is approximately 8 kg, and two-piece aprons can weigh up to

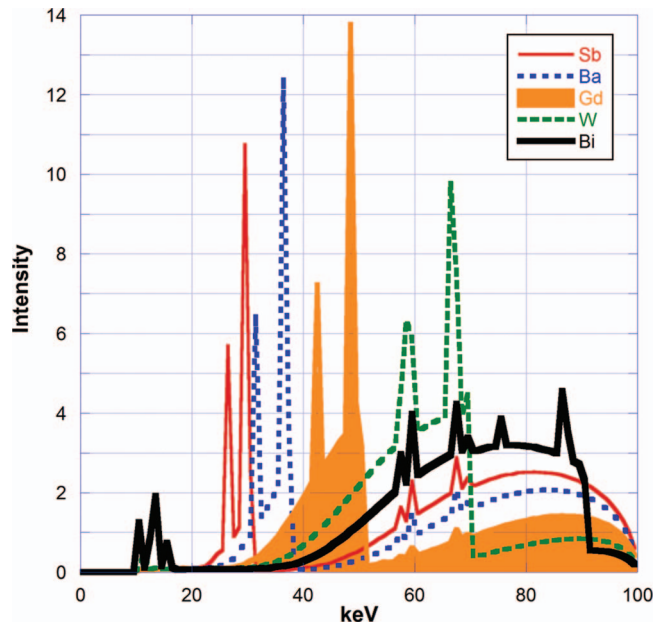


FIG. 2. Monte Carlo calculated transmission spectra resulting from 0.25 mm Pb equivalent attenuation of a 100 kVp x-ray beam by several non-Pb metals in use in radiation protection materials. The Bi spectrum is very similar to Pb.

10 kg.²⁸ Although most regulatory agencies call for 0.5 mm Pb equivalent protection, in situations such as IR where individuals stand for long hours, choosing the appropriate level of radiation protection based on relevant radiation ranges minimizes the weight, discomfort, and fatigue resulting from the use of radiation shielding garments, and can prevent possible longer term musculoskeletal problems.^{11,28}

Utilizing non-Pb materials, the K-absorption edge behavior provides an opportunity to target radiation ranges and lower the weight of radiation protection garments. However, a problem arises from the enhanced fluence due to fluorescence below each element's K-absorption edge (discussed below). Figure 2 displays MC calculated spectra resulting from 0.25 mm Pb-equivalent attenuation by several non-Pb metals [the attenuated spectrum of Pb ($Z = 82$, not shown) is very similar to Bi ($Z = 83$)]. All of the spectra retain traces of the $K\alpha$ and $K\beta$ emission peaks for W at 59 and 67 keV resulting from the use of a W anode in the x-ray tube. The elements with K-absorption edges slightly below the W peaks are very effective at attenuating these emission lines—note in Fig. 2 the filled Gd spectrum and the highly attenuated W emission peaks. Ba and to a lesser degree Sb are also effective in this regard. Different metals provide more effective attenuation in different energy ranges, as observable in Fig. 2. An opportunity therefore exists for improving attenuation capabilities per unit weight through the use of bilayers, where the second layer compensates for the fluorescence from the first layer.

Figure 3 displays MC-calculated attenuation effects of equivalent radiological thicknesses of pure metal layers of Ba, Bi, and a bilayer of Ba + Bi when irradiated with the ASTM 100 kVp, HVL 5.2 mm Al, x-ray quality. The sharp peaks in the 100 kVp spectra as well as the Ba, Bi, and Ba + Bi spectra in Figs. 3(a)–3(d) are the $K\alpha$ and $K\beta$ emission peaks for W at

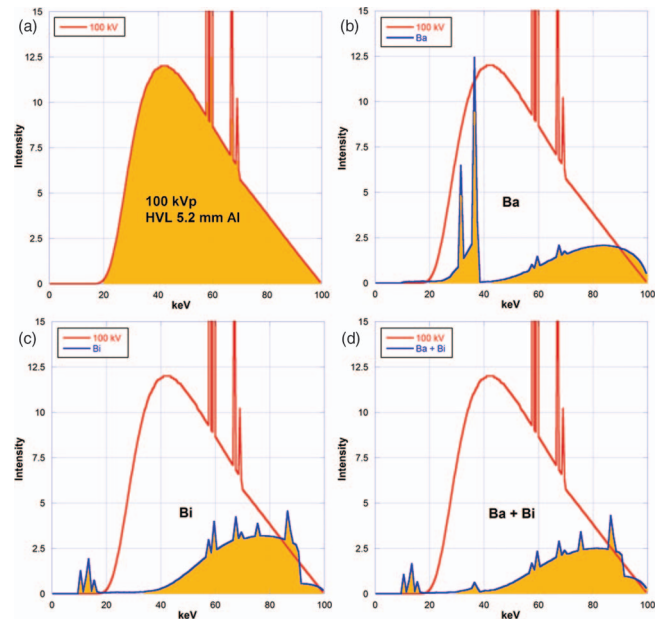


FIG. 3. MC-calculated attenuated spectra of equivalent radiological thicknesses of pure metal layers of (b) Ba, (c) Bi, and a bilayer of (d) Ba + Bi for the (a) ASTM 100 kVp x-ray quality (a).

59 and 67 keV. The Ba, Bi, and Ba + Bi spectra are all to the same scale for comparison, but the 100 kVp spectrum is not to scale and is included only to demonstrate the contrast between the initial and final spectral shapes resulting from attenuation of this spectrum by these metal layers.

In Fig. 3, the Ba layer [Fig. 3(b)] demonstrates effective attenuation in the 40–100 kV range but at the expense of the photoelectric effects below the K-absorption edge at approximately 37.5 keV and the $K\alpha$ and $K\beta$ emission peaks of Ba at 32 and 36 keV. The Bi layer [Fig. 3(c)] provides effective attenuation below 40 keV with only small $L\alpha$ and $L\beta$ emission peaks at 11 and 13 keV, and small $K\alpha$ and $K\beta$ emission peaks at 76 and 87 keV. By creating a bilayer [Fig. 3(d)] with half the radiological thickness composed of Ba (upstream, closest to the x-ray tube) and the other half the thickness composed of Bi (downstream), the complimentary effects of the two materials result in increased total attenuation since the Bi layer will attenuate the characteristic $K\alpha$ and $K\beta$ x rays emitted by the Ba. The radiological thickness¹⁹ can be obtained by multiplying the density of the material by the measured layer thickness to obtain a measurement in units of g/cm^2 .

This low Z upstream/high Z downstream bilayer configuration is effective with many combinations of materials.²⁰ However, these calculations assumed that layers of pure metal are being utilized, since the exact composition of these proprietary materials was not available. The actual attenuating performance per unit weight of manufactured radiation protection materials is diminished by the added weight contribution of the polymer material in which the metal powder is embedded, and if the metal is a component of a compound, additional degradation of performance results from the weight of the nonmetal components of the compound. Therefore, accurate characterization of any radiation attenuation material

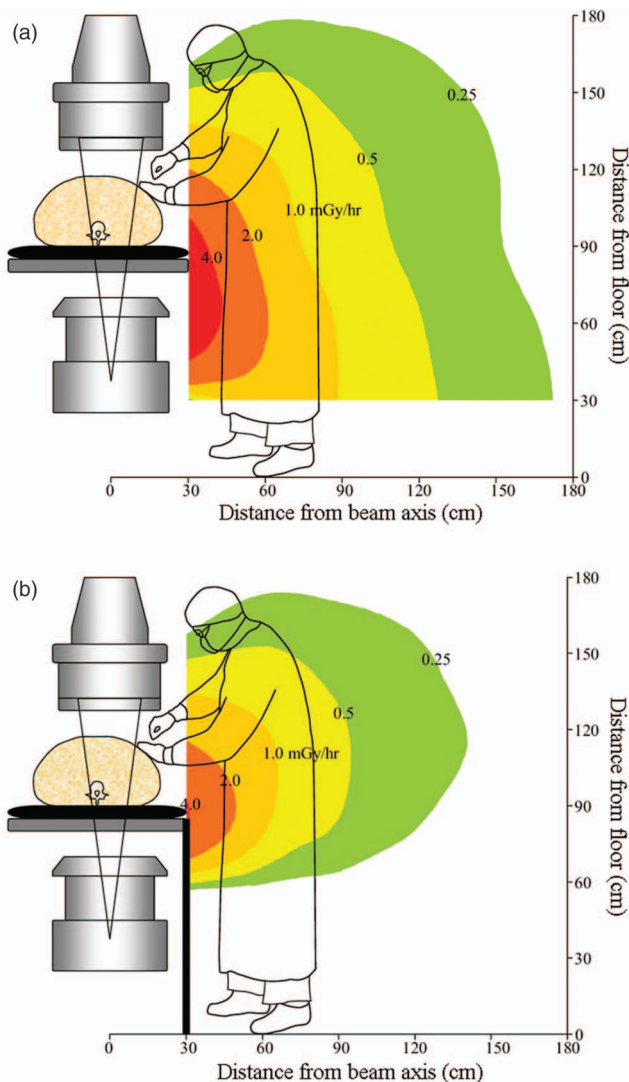


FIG. 4. (a) The distribution of x-ray scatter [from measurements conducted at the Mayo Clinic (Ref. 29) with permission]. (b) The distribution of x-ray scatter with undertable shielding in place.

requires attenuation measurements with the actual material at appropriate x-ray qualities.

IR physicians wear radiation shielding garments to reduce the real and perceived radiation risk,⁹ and are rarely exposed to the primary x-ray beam with the possible exception of their hands. However, IR personnel are exposed to a significant quantity of scattered radiation, which is almost entirely attributable to scatter from the patient and objects exposed to the primary beam.^{9,29} The distribution of this scatter is illustrated in Figs. 4(a) and 4(b) (from measurements conducted at the Mayo Clinic,²⁹ with permission). With undertable shielding in place, the scatter is dramatically decreased [Fig. 4(b)], but a significant amount still originates from the patient. The maximum intensity can be approximated as scatter at 90° to the incident beam, as illustrated in these figures.

In defining kVp ranges in Standards, which evaluate the effectiveness of radiation attenuation garments, the kVp of the scattered radiation should be the x-ray beam quality of interest. The kVp of this scattered radiation is significantly less

than the incident kVp, due to Compton scattering. Recognition of this fact provides a real benefit for IR personnel in that lighter-weight garments would then be recognized as compliant with the Standards requirements. Non-Pb materials can provide superior attenuation at lower kVp ranges, resulting in lighter materials. However, (except for Bi) they can be less effective attenuators than Pb at the highest kVp ranges, requiring heavier materials for equivalent attenuation.¹⁹

The purpose of this study is to investigate three aspects for improving the effectiveness and reducing the weight of radiation attenuating materials:

- the relative merits of the different measurement geometries detailed in the three Standards listed above,
- radiation attenuation characteristics of new materials based on Ba, Gd, and Bi compounds,
- realistic kV range requirements in Standards based on the scattered spectra.

II. METHODS

II.A. Measurement geometry—non-Pb compounds

The three Standards^{22–24} listed in the Introduction all recommend different measurement geometries for characterizing radiation protection materials. ASTM F2547-06 recommends a setup where the distance from the x-ray tube focal spot to the detector is 1000 mm, with the radiation attenuation material positioned 400 mm from the focal spot. This is referred to as “narrow beam geometry,” and does not include the effects of secondary radiation from the attenuation material (scatter and fluorescence) in the measurement (see Fig. 5). This secondary component is significant when wearing a radiation protection garment close to the skin. The DIN 6857 Standard recommends an “inverse broad beam geometry,” where the radiation attenuation material is mounted directly behind a 4 mm thick Pb aperture, and the detector is mounted directly behind this material. Measurements made in this geometry include scatter and fluorescence from the radiation attenuation material. In this study, we will refer to the geometry where the attenuating material is approximately halfway between the x-ray focal spot and the detector as “narrow beam geometry,” and where the attenuation material is sandwiched between an aperture and the detector as “broad beam geometry”. The IEC 61331-1 Standard provides for both a narrow beam and broad beam geometry, but in both cases there is a ≥ 50 mm gap between the radiation attenuation material and the detector, thereby excluding some of the scattered and fluorescent radiation in the broad beam measurement. For all measurements described in this paper, a broad beam geometry was used, similar to that described in DIN 6857 and illustrated in Fig. 5.

II.B. Measurement geometry—scatter

IR personnel are rarely exposed to the primary x-ray beam but receive a significant quantity of scattered radiation, which is almost entirely attributable to scatter from the patient and objects exposed to the primary beam. To approximate these scatter conditions, an International Organization for

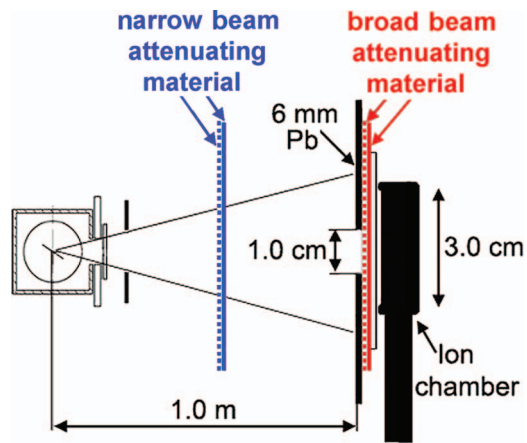


FIG. 5. The geometrical positioning of attenuating material for narrow beam vs broad beam measurements.

Standardization water slab phantom (30 cm \times 30 cm \times 15 cm) (Ref. 30) was placed at a 45° angle to the incident x-ray beam, so that the center of the front face of the phantom was located 1.0 m from the x-ray tube anode. For these measurements, the incident x-ray beams that were utilized were the eight ASTM x-ray qualities from 60 to 130 kVp.²² A second water phantom (30 cm \times 30 cm \times 30 cm) was positioned so that the center of the front face of this second phantom was 0.5 m from the center of the first phantom, perpendicular to the incident beam. The detector was mounted directly against this second phantom to include backscatter. Figure 6 illustrates this setup with an annotated simulation geometry which was used for the subsequent Monte Carlo modeling.

II.C. Monte Carlo calculations

MC calculations were performed for the two measurement geometries in Sec. II. The first set of calculations approximated the setup shown in Fig. 5 for broad beam attenuating

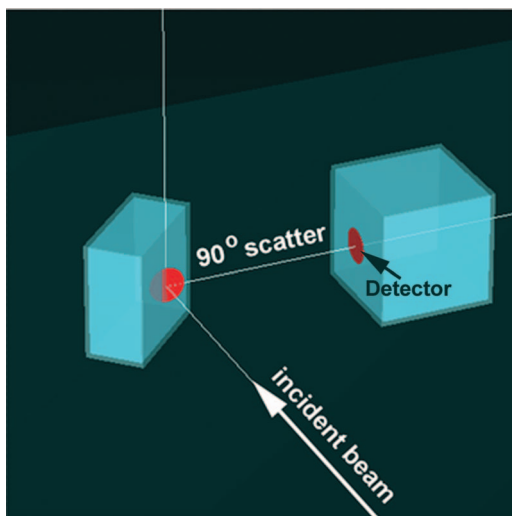


FIG. 6. The 90° scatter geometry utilized for measurements and MC calculations to determine the differences in spectra between the direct and scattered ASTM beams.

material, as discussed in Ref. 20. A second set of MC results were acquired by calculating the resulting spectra after a primary x-ray beam was scattered at 90° by a water phantom placed at 45° to the incident x-ray beam, and subsequently backscattered by a second water phantom (Fig. 6). This geometry was used to simulate the situation where an IR physician is subjected to scattered radiation from a patient. The EGSnrc MC user codes *BEAMnrc* and *cavity* were used to model this scatter, and reproduced the measured results. The simulations proceeded in two stages. First, the relevant NRC x-ray tube and appropriate filtration for the ASTM x-ray qualities were modeled using *BEAMnrc* to generate “photon sources” at a point beyond the filtration for each quality. These “photon sources” were then used in the user code *cavity* as the spectra of the incident photons. After transport through the phantom geometry, the resulting spectra of the photons crossing the detector plane were recorded. Finally, a “surrogate spectrum” was determined that matched the HVL and the kVp (to the nearest 5 kV) of these resulting spectra.

III. RESULTS

III.A. Measurement geometry

In interventional radiology, the x-ray tube accelerating voltage is typically less than 90 kVp. Fluorescent radiation from Pb-based (or Bi-based) materials is therefore minimal due to the relatively high energy of the K-absorption edges (approximately 88 keV for Pb and 90.5 keV for Bi). However, fluorescence is significant for metals with lower Z such as Sb, Sn or W, commonly used in non-Pb radiation attenuation garments. In these cases, the x-ray fluorescence radiation generated by these materials can make a significant contribution to the total radiation reaching the individual. All measurements of attenuation by radiation shielding materials undertaken in this study employed the broad beam geometry described in Sec. II. To demonstrate the difference in attenuation that can occur with narrow beam versus broad beam measurement geometries, Fig. 7 shows the results of measurements of a commercial Sb-loaded radiation attenuating material which was irradiated with the 70 kVp ASTM x-ray quality and measured in the narrow beam and broad beam configurations (Fig. 5). The difference in air kerma measurements between these two geometries corresponds to a weight difference of 14% and 25% for 0.5 mm Pb equivalent and 0.25 mm Pb equivalent material requirements, respectively. While this example only applies to this particular Sb-based material at the 70 kVp ASTM quality, it demonstrates that the broad beam geometry provides a more appropriate measure of attenuation by radiation shielding materials.

III.B. Non-Pb compounds

Non-Pb radiation attenuation materials have typically been composed of pure metal powders such as Sb, Sn, and W imbedded in a polymer matrix. Recently, several manufacturers have experimented with materials incorporating metallic compounds such as BaSO₄, Gd₂O₃, and Bi₂O₃. The

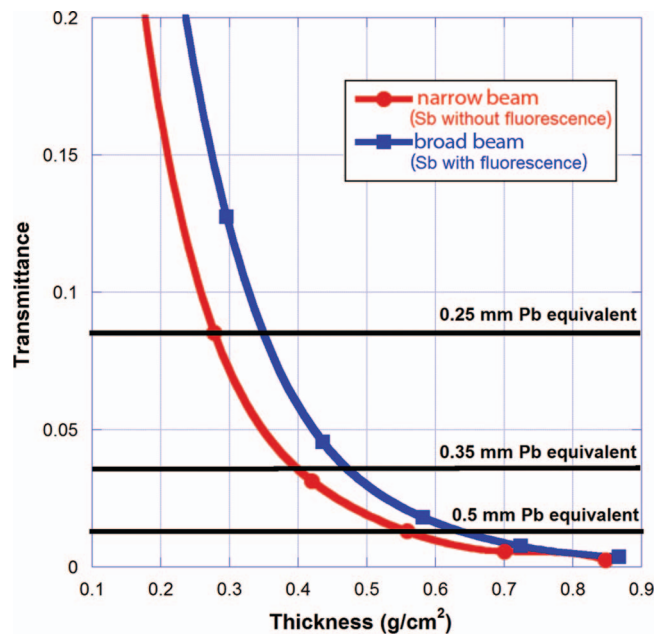


FIG. 7. Commercial Sb-loaded radiation attenuating material irradiated with the 70 kVp ASTM x-ray quality and measured in the narrow beam (without fluorescence) and broad beam (with fluorescence) geometries.

relative weight of the metal atoms in the BaSO_4 , Gd_2O_3 , and Bi_2O_3 compounds is approximately 59%, 87%, and 90%, respectively. The sulphur and oxygen in these compounds add weight but do not contribute significantly to the attenuation capabilities of the material. Nonetheless, the high percentage of metal, particularly for Gd_2O_3 and Bi_2O_3 , suggested that these materials were worthy of investigation.

MC calculations for the attenuating capabilities of a Ba + Bi bilayer combination were performed in an earlier study.²⁰ While no manufactured materials containing these metals were available for measurements at that time, the MC calculations showed that this bilayer combination should perform significantly better and more consistently than the other combinations modeled and measured. Since the earlier studies, several manufacturers have produced experimental material containing compounds incorporating these metals. Figure 8 displays transmission vs thickness measurements of several of these experimental materials under irradiation in the broad beam geometry utilizing the 100 kVp ASTM x-ray quality. The most challenging x-ray qualities for attenuation by non-Pb materials are the higher kVp qualities, where typically non-Pb materials perform much less effectively than the Pb-based materials.^{19,20} Included in Fig. 8 are individual measurements performed for the three compounds mentioned above, pure Pb, a commercial Pb apron material, and bilayers arranged so that the lower Z compound materials (BaSO_4 and Gd_2O_3) were upstream and the high Z material (Bi_2O_3) was downstream in the x-ray beam. The BaSO_4 layer (labeled “Ba”) showed the highest transmission (lowest attenuation) per unit weight primarily due to the fact that the weight% of Ba in the compound was only 59%. The Gd_2O_3 -based material (labeled “Gd”) performed better than the BaSO_4 -based material. The Bi_2O_3 material (labeled “Bi”)

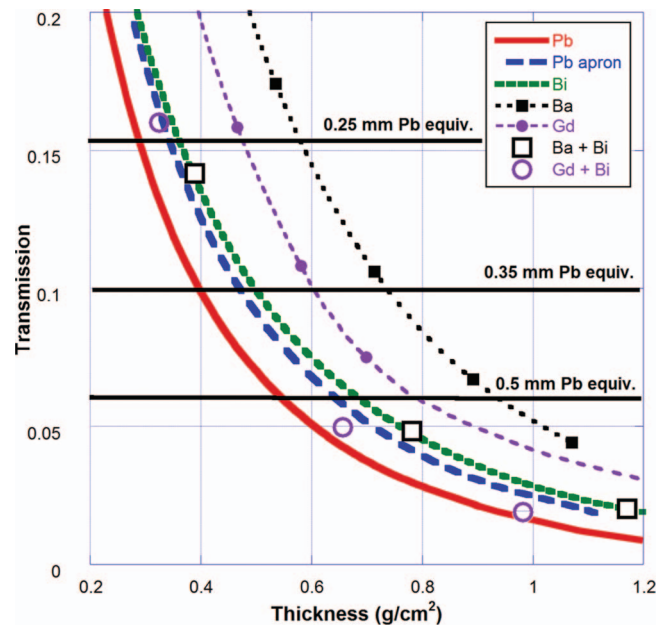


FIG. 8. Transmission vs thickness measurements of several experimental materials and bilayers, irradiated in the broad beam geometry with the 100 kVp ASTM x-ray quality.

performed the best of the compound materials, and almost as well as the commercial Pb-based material (“Pb apron”) in spite of the fact that Bi composed only 90% of the weight of the Bi_2O_3 material. Use of pure metal Bi powder rather than Bi_2O_3 in an experimental material developed by another manufacturer³¹ showed results (not included here) where the material matched the attenuation capabilities of the Pb apron material.

Two bilayers were also measured. The bilayer of BaSO_4 and Bi_2O_3 (large open squares: “Ba + Bi”) performed as well as the equivalent thickness of Bi_2O_3 . Since BaSO_4 costs only 10% as much as Bi_2O_3 , this offers a more economical and equally effective alternative to garments constructed from the Bi_2O_3 material only. The bilayer of Gd_2O_3 and Bi_2O_3 (large open circles: “Gd + Bi”) provided more attenuation than the commercial Pb apron material, and approached the performance of pure Pb. The measurements made here at the 100 kVp ASTM quality demonstrate that materials incorporating these two bilayer combinations provide similar attenuation as Pb-based materials due to the inclusion of Bi, which has very similar attenuating properties to Pb. Coupled with the superior attenuating performance at the lower kVp qualities shown by MC calculations,²⁰ these two bilayer combinations show promise of superior radiation attenuation per unit weight for commercial radiation protection materials.

Figure 8 can be used to determine the relative weights of radiation protection garments made with these materials. To compare the attenuation capabilities of 0.35 mm Pb equivalent materials, for example, thickness values in g/cm^2 can be interpolated from each of the curves. If we assign a weight of 1.0 to the commercial Pb-based material (“Pb apron”), a pure Pb garment would weigh 0.84, the Gd + Bi bilayer would weigh 0.97, the Bi_2O_3 material and the Ba + Bi bilayer would

both weigh 1.06, and the Gd_2O_3 and BaSO_4 materials would weigh 1.29 and 1.57, respectively.

III.C. Bi_2O_3 -loaded hand cream

Discussions of radiation attenuation materials typically focus on the torso or thyroid, where sheets of material can be formed to provide appropriate protective garments. However, hand doses can be substantially higher than that received by the neck or torso, since fingers can be exposed directly to the primary entrance or exit beams, in addition to exposure to the highest scatter rates due to proximity to the patient. Pb- or Bi_2O_3 -loaded latex gloves are commercially available to IR physicians for hand protection. These glove materials typically offer substantially less protection than the radiation attenuating material incorporated into garments such as aprons due to the practical requirements for gloves to be constructed of stretchable material that is light and pliable enough to not interfere with dexterity. Because of toxicity, Bi is a good choice as a replacement for Pb as it is not known to be a significant threat to the environment, is poorly absorbed and is relatively nontoxic by inhalation or ingestion. Bi is not considered a human carcinogen.

A novel approach to radiation protection for the hands is the recent development of a Bi_2O_3 -loaded cream^{21,32} which is designed to be spread either on bare or gloved hands, dry quickly, and subsequently be covered with a (second) surgical glove to provide containment of the material. Removal of the gloves removes the dry Bi_2O_3 cream layer with any remaining residue washed off with water. Figure 9 shows a comparison of the relative effectiveness of this new Bi_2O_3 -loaded cream to a commercial Bi_2O_3 -loaded glove. As expected, the cream provides better protection than the glove material on a per unit mass basis. However, the thickness and consistency achieved

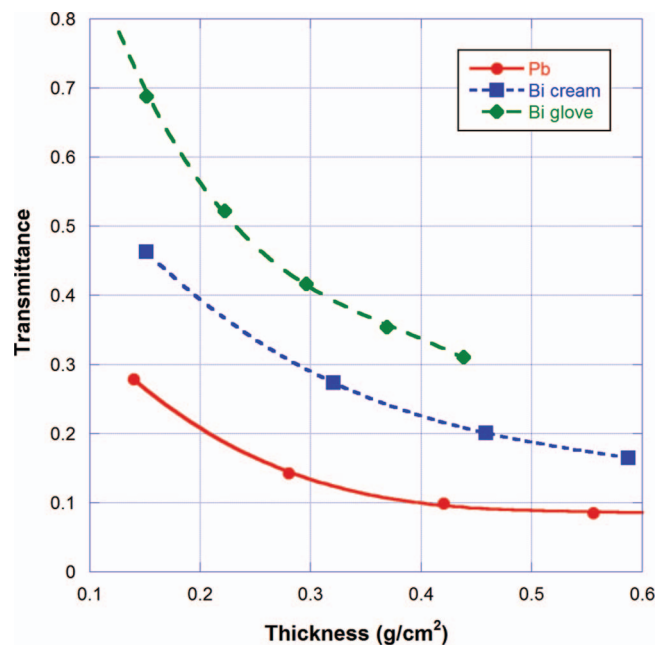


FIG. 9. Comparison of the relative effectiveness of a Bi_2O_3 -loaded hand cream to a commercial Bi_2O_3 -loaded glove, with reference to pure Pb.

in an application of this cream is likely to vary by individual and even by application. In any case, the protection provided by either gloves or cream is likely to be less than the 0.5 mm Pb equivalent desired. The issue of how best to protect the hands of IR physicians is under consideration as the topic of a follow-up study.

III.D. Surrogate x-ray qualities based on scatter

Cardiac-catheterization-fluoro systems used by IR personnel usually have a maximum operating voltage in the range from 100 to 125 kVp, and the actual operating voltage is continuously adjusted by automatic dose rate control (ADC) circuitry.⁹ IR personnel are rarely exposed to the primary x-ray beam but receive a significant quantity of scattered radiation, which is almost entirely attributable to scatter from the patient and objects exposed to the primary beam. To study this scatter and to accommodate the 100–125 kVp range as well as the lower kVp ranges, we performed a series of 90° scatter measurements and Monte Carlo calculations using the eight ASTM x-ray qualities from 60 to 130 kVp, for the purpose of determining the difference in spectra between the direct and scattered ASTM beams. Figure 6 illustrates this setup with an annotated simulation geometry which was used for the Monte Carlo modeling.

As an example of the change in an incident x-ray spectrum after scatter, in Fig. 10 the spectral shapes of the ASTM 100 kVp spectrum, the 90° scattered spectrum, and a conservative 80 kVp “surrogate” spectrum are shown. The scattered spectrum was measured as having approximately 1.1% the air kerma of the incident spectra but is shown magnified in Fig. 10 to allow comparisons of the spectral shapes. The surrogate spectrum does not accurately match the scattered spectrum but approximates the kVp and matches the HVL. In this

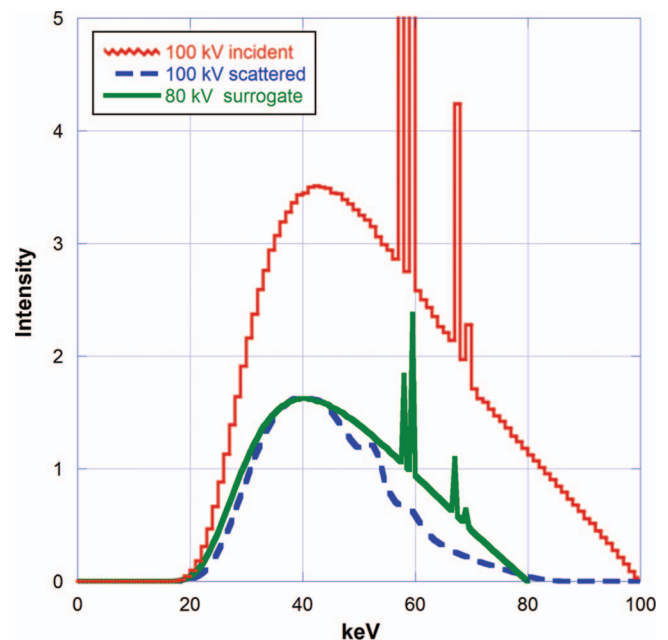


FIG. 10. ASTM 100 kVp spectra shown with the MC-calculated 90° scattered spectra plus a HVL-matched “surrogate” x-ray quality spectra.

TABLE I. ASTM F2547-06 Standard x-ray qualities (columns 1 and 2), and surrogate x-ray qualities (columns 3 and 4) based on MC-calculated spectra resulting from 90° scatter.

ASTM F2547-06 x-ray qualities		90° scatter surrogate qualities (approximate)	
kVp	HVL (mm Al)	kVp	HVL (mm Al)
60	2.9	50	2.6
70	3.3	60	2.9
80	4.0	70	3.4
90	4.3	75	3.7
100	5.2	85	4.0
110	5.5	90	4.3
120	6.3	100	4.5
130	6.7	105	5.1

way, it provides a reasonable approximation of the scattered spectrum in a form that can be easily duplicated for testing and measurements.

A full set of the eight ASTM qualities were modeled, the incident spectra and scattered spectra were determined, and surrogate spectra were matched to the scattered spectra. The results are shown in Table I and show that the highest kVp qualities produce scattered surrogate qualities with kVps approximately 20 kV less than the incident beams. Also, all surrogate spectra are “softer,” i.e., have lower HVLs, than the incident beams. These calculations demonstrate that the highest kVp x-ray quality for a Standard addressing attenuation by non-Pb radiation protection materials for IR personnel could realistically be set at 100 kVp with a HVL of 4.5 mm Al. The attenuation by 0.5 mm of Pb in this beam is slightly better than 95%. This leads to a further suggestion that if an alternative to the Pb-equivalent scale were desired, a requirement such as “95% attenuation (5% transmission) at 100 kVp HVL 4.5 mm Al” would be a reasonable benchmark.

IV. CONCLUSIONS

Broad beam geometry is a measurement setup where the detector is mounted against the downstream side of attenuating materials undergoing testing, thereby including fluorescent radiation from the material itself in the measurement. This geometry provides a more realistic measure of the attenuating characteristics of radiation protection materials, and was used throughout this study. For non-Pb materials, the difference in attenuation between broad beam and narrow beam (fluorescence not included) geometries can vary significantly. For example, for Sb-based material measured at the 70 kVp ASTM quality, broad beam vs narrow beam geometries produce differences in weight ranging from 14% to 25% for 0.5 mm Pb equivalent and 0.25 mm Pb equivalent material, respectively.

Materials incorporating metallic compounds such as BaSO₄, Gd₂O₃, and Bi₂O₃ were characterized and found to perform almost as effectively as materials incorporating pure metal powders, even though the relative weight of the metal

atoms in these three compounds is approximately 59%, 87%, and 90% for Ba, Gd, and Bi respectively. Bilayers ordered with the low-Z layer upstream (BaSO₄ or Gd₂O₃ closest to the radiation source) and the high-Z layer downstream (Bi₂O₃ closest to the person or detector) provide very efficient attenuation. Because of the influence of the photoelectric effect, the weight of non-Pb materials that provides Pb-equivalent protection varies with the photon energy. In particular, non-Pb materials can offer substantial improvement in attenuation over Pb-based materials in the energy range above the K-absorption edge of the metal component, and bilayers can extend this improvement to lower energies. Materials incorporating Bi₂O₃ offer a particular advantage because these materials provide very similar attenuation to Pb-based materials, making the match to Pb-equivalent guidelines simpler and more consistent than for other commonly utilized non-Pb materials. When Bi₂O₃ is used as the high-Z component in a bilayer, the performance is particularly effective. Of particular note concerning the attenuating effectiveness of Bi₂O₃ is the recent development of a Bi₂O₃-based hand cream that shows potential for improved hand protection for IR personnel.

IR personnel are rarely exposed to the primary x-ray beam but are instead exposed to significant levels of scattered radiation, attributable to scatter from the patient and objects exposed to the primary beam. Measurements and MC calculations demonstrated that the kVp of the scattered radiation is significantly less than the kVp of the incident beam, varying from a difference of 10 kVp at the ASTM 60 kVp x-ray quality up to 25 kVp at the ASTM 130 kVp x-ray quality. A table of surrogate x-ray qualities was calculated, approximating the resulting x-ray qualities after 90° scatter of the eight ASTM F2547-06 Standard x-ray beams. As an alternative to the Pb-equivalent method of comparison for radiation protection materials, a protocol requiring ≥95% attenuation (≤5% transmission) at the 100 kVp, HVL 4.5 mm Al x-ray beam quality is suggested.

ACKNOWLEDGMENTS

The authors acknowledge helpful discussions with Carl Ross, National Research Council of Canada (NRC) and Thomas Beck, Beck Radiological Innovations, Inc. The authors are grateful for access to experimental and commercial radiation attenuating materials provided by BloXR Corp. and Beck Radiological Innovations, Inc. (Bar-Ray material). J.P.M. wishes to acknowledge Martin Lilly, Lite Tech Inc., whose comments and insights initiated this work five years ago.

^{a)} Author to whom correspondence should be addressed. Electronic mail: john.mccaffrey@nrc-cnrc.gc.ca

¹ B. J. McParland, J. Nosil, and B. Burry “A survey of the radiation exposures received by the staff at two cardiac catheterization laboratories,” *Br. J. Radiol.* **63**, 885–888 (1990).

² L. Renaud “A 5-y follow-up of the radiation exposure to in-room personnel during cardiac catheterization,” *Health Phys.* **62**(1), 10–15 (1992).

³ M. Zuguchi, K. Chida, M. Raura, Y. Inaba, A. Ebata, and S. Yamada “Usefulness of non-lead aprons for radiation protection of physicians per-

- forming interventional procedures," *Radiat. Prot. Dosim.* **131**(4), 531–534 (2008).
- ⁴S. Kim, T. T. Yoshizumi, D. P. Frush, C. Anderson-Evans, and G. Tonehava, "Dosimetric characterization of bismuth shields in CT: measurements and Monte Carlo simulations," *Radiat. Prot. Dosim.* **133**, 105–110 (2009).
- ⁵K. P. Kim, D. L. Miller, S. Balter, R. A. Kleinerman, M. S. Linet, D. Kwon, and S. L. Simon "Occupational radiation doses to operators performing cardiac catheterization procedures," *Health Phys.* **94**(3), 211–227 (2008).
- ⁶K. P. Kim and D. L. Miller, "Minimizing radiation exposure to physicians performing fluoroscopically guided cardiac catheterization procedures: a review," *Radiat. Prot. Dosim.* **133**(4), 227–233 (2009).
- ⁷J. R. Williams, "The interdependence of staff and patient doses in interventional radiology," *Br. J. Radiol.* **70**, 498–503 (1997).
- ⁸K. Chida, Y. Morishima, Y. Inaba, M. Taura, A. Ebata, K. Takeda, H. Shimura, and M. Zuguchi, "Physician-received scatter radiation with angiography systems used for interventional radiology: Comparison among many X-ray systems," *Radiat. Prot. Dosim.* **149**(4), 410–416 (2011).
- ⁹S. Balter, "Stray radiation in the cardiac catheterization laboratory," *Radiat. Prot. Dosim.* **94**(1–2), 183–188 (2001).
- ¹⁰K. Chida, M. Kato, H. Saito, T. Ishibashi, S. Takahashi, M. Kohzuki, and M. Zuguchi, "Optimizing patient radiation dose in intervention procedures," *Acta Radiol.* **51**, 33–39 (2010).
- ¹¹N. Papadopoulos, C. Papaefstathiou, P. A. Kaplanis, G. Menikou, G. Kokona, D. Kaolis, C. Yiannakaras, and S. Christofides, "Comparison of lead-free and conventional x-ray aprons for diagnostic radiology," in *WC2009, IFMBE Proceedings 25/III*, edited by O. Dossel and W. C. Schlegel (Springer, Berlin, 2009), pp. 544–546.
- ¹²E. W. Webster, "Experiments with medium Z materials for shielding against low-energy X-rays," *Radiology* **86**, 146 (1966).
- ¹³M. J. Yaffe, G. E. Mawdsley, L. Martin, R. Servant, and R. George, "Composite materials for X-ray protection," *Health Phys.* **60**, 661–664 (1991).
- ¹⁴E. W. Webster, "Addendum to 'Composite materials for X-ray protection'," *Health Phys.* **61**, 917–918 (1991).
- ¹⁵P. H. Murphy, Y. Wu, and S. A. Glaze, *Radiology* **186**, 269–272 (1993).
- ¹⁶P. J. Kicken, and A. J. J. Bos, "Effectiveness of lead aprons in vascular radiology: results of clinical measurements," *Radiology* **197**, 473–478 (1995).
- ¹⁷E. G. Christodoulou, M. M. Goodsitt, S. C. Larson, K. L. Darner, J. Satti, and H.-P. Chan, "Evaluation of the transmitted exposure through lead equivalent aprons used in a radiology department, including contribution from backscatter," *Med. Phys.* **30**, 1033–1038 (2003).
- ¹⁸Y. Takano, K. Okazaki, K. Ono, and M. Kai, "Experimental and theoretical studies on radiation protective effect of a lighter non-lead protective apron," *Nippon Hoshasen Gijutsu Gakkai Zasshi (Jpn. J. Radiol. Technol.)* **61**, 1027–1032 (2005) (in Japanese).
- ¹⁹J. P. McCaffrey, H. Shen, B. Downton, and E. Mainegra-Hing, "Radiation attenuation by lead and nonlead materials used in radiation shielding garments," *Med. Phys.* **34**(2), 530–537 (2007).
- ²⁰J. P. McCaffrey, E. Mainegra-Hing, and H. Shen, "Optimizing non-Pb radiation shielding materials using bi-layers," *Med. Phys.* **36**(12), 5586–5594 (2009).
- ²¹BloXR Corp., Salt Lake City, UT.
- ²²*ASTM F 2547-06: Standard Test Method for Determining the Attenuation Properties in a Primary X-ray Beam of Materials Used to Protect Against Radiation Generated During the Use of X-ray Equipment*, ASTM International, West Conshohocken, PA, 2006.
- ²³*DIN 6857: Radiation Protection Accessories for Medical Use of X-rays—Part 1: Determination of Shielding Properties of Unleaded or Lead Reduced Protective Clothing*, Normenausschuss Radiologie (NAR) im DIN, Radiology Standard Committee within the DIN institute, 2007.
- ²⁴*IEC 61331-1: Protective Devices Against Diagnostic Medical X-radiation—Part 1: Determination of Attenuation Properties of Materials*, Bureau Central de la Commission Electrotechnique Internationale, Genève, Suisse, 1994.
- ²⁵I. Kawrakow, E. Mainegra-Hing, D. W. O. Rogers, F. Tessier, and B. R. B. Walters, "The EGSnrc Code System: Monte Carlo Simulation of electron and photon transport," NRC Report PIRS 701, Ottawa, 2011 (available URL: <http://irs.inms.nrc.ca/software/egsnrc/documentation/pirs701.pdf>).
- ²⁶D. W. O. Rogers, B. R. B. Walters, and I. Kawrakow, "BEAMnrc Users Manual," NRC Report PIRS 509, Ottawa, 2011 (available URL: <http://irs.inms.nrc.ca/software/beamnrc/documentation/pirs0509/index.html>).
- ²⁷*Radiation Oncology Physics: A Handbook for Teachers and Students*, edited by E. B. Podgorsak (IAEA, Vienna, 2005).
- ²⁸A. M. Ross, J. Segal, D. Borenstein, E. Jenkins, and S. Cho, "Prevalence of spinal disc disease among interventional cardiologists," *Am. J. Cardiol.* **79**(1), 68–70 (1997).
- ²⁹T. J. Vrieze, B. A. Schueler, H. Bjarnason, and A. W. Stanson, "An investigation of operator exposure in interventional radiology," *Radiology* **225**(P), 713 (2002).
- ³⁰International Organization for Standardization, "X and gamma reference radiation for calibrating dosimeters and for determining their response as a function of photon energy—Part 3: Calibration of area and personal dosimeters and the measurement of their response as a function of energy and angle of incidence," International Organization for Standardization 4037–3, 1999.
- ³¹Bar-Ray Products, Littlestown, PA.
- ³²S. S. Shaw, K. W. Chen, and A. Mejia, "Radiation protection to surgeons' hands with a novel radiation attenuating lotion," presented at the 2012 AAOS Annual Meeting: Scientific SE39, February 7–11, 2012.